Vol. 47, No. 3 (2025) 414-425, DOI: 10.24874/ti.1931.04.25.07

Tribology in Industry

www.tribology.rs

RESEARCH

Minimizing Cam Surface Deformation Using Modified Geometry Under Point Contact Elastohydrodynamic Lubrication

Amjad Al-Hamood[a], Zahraa Al-Dujaili[a], Moneer Tolephih[b], Hakim S. Sultan Aljibori[c], Hazim Jamali[a], Oday Abdullah[d,e,f], Nadica Stojanovic[g,*]

[a]*Mechanical Engineering Department, College of Engineering, University of Kerbala, Karbala, Iraq*
[b]*Al-Naji University, Baghdad, Iraq,*
[c]*College of Engineering, University of Warith Al-Anbiyaa, Karbala, Iraq,*
[d]*Department of Energy Engineering, College of Engineering, University of Baghdad, Iraq,*
[e]*College of Engineering, Al-Naji University, Baghdad, Iraq,*
[f]*Department of Mechanics, Al-Farabi Kazakh National University, Almaty, Kazakhstan,*
[g]*Faculty of Engineering, University of Kragujevac, Kragujevac, Serbia.*

Keywords:

Cam
Flat follower
Modified depth
Surface deformation
EHL

* Corresponding author:

Nadica Stojanovic
E-mail: nadica.stojanovic@kg.ac.rs

Received: 7 April 2025
Revised: 28 May 2025
Accepted: 15 July 2025

A B S T R A C T

The cam and follower mechanism is commonly used in converting rotational motion into reciprocating motion in a large variety of applications. In general, the contact between the cam and its follower is a non-conformal contact, which results in an elastohydrodynamic lubrication contact regime. In this study, the elastohydrodynamic lubrication problem of the cam and flat-faced follower is investigated in order to reduce the elastic deformation of the contacting surfaces based on using different surface geometries. The effects of using three forms of transverse geometrical modifications are investigated, which are whole parabolic depth, linear chamfer, and parabolic chamfer. The contact problem is solved numerically using the differential deflection coupled method based on the finite difference method. The solution involves the determination of the radius of relative curvature, the load, and the surface velocities at the contact point. The results show that the surface deformation is affected significantly by the type of modification. The parabolic chamfer is the best form in minimizing the surface deformation, resulting in about 3.8 μm maximum deformation in comparison with 4.3 μm and 5.1 μm when the linear chamfer and whole parabolic profile are used, respectively. Furthermore, the parabolic chamfer reduces the maximum pressure value significantly.

1. INTRODUCTION

Cam-follower is a simple mechanism that converts rotational motion into reciprocating motion (or rarely oscillatory motion). This mechanism has fewer parts, needs a smaller room, is less expensive, and is more reliable. These features make it widely used in the timing

of a large variety of machinery like printing, paper cutting, packaging, spinning, and weaving textiles. They are most commonly used in internal combustion engines for managing valve timing. The desired function of the cam-follower mechanism depends mainly on follower type and cam profile. The cam profile is either selected from the very common profile types or designed for a more specific function. The follower types are commonly classified according to their contact geometry, like; flat face, curved face, and knife edge. Further readings about cam profiles and follower types are available in Rothbart [1].

In general, the contact between the cam and its follower is considered as non-conformal, where it is either line or point contact, which is similar to the contact at mating teeth in gears and roller bearings. On the other hand, when surface contact develops between bodies, like in a journal bearing, it is considered as a conformal contact. When a proper lubricant exists between the non-conformal surfaces during operation, fluid film develops, and significant surface deformation occurs, the lubrication is known as elastohydrodynamic lubrication (EHL). In machines, lubrication of moving parts is very important to reduce wear in its parts, which extends the machine's life. Furthermore, lubrication reduces friction between these parts, which leads to lower power loss, reduction in fuel consumption, and pollution. The cam follower mechanism represents a major part in internal combustion engines; it needs to be lubricated efficiently for the reasons mentioned.

Dyson and Naylor [2] carried out an earlier study on cam lubrication focusing on tapped distresses like scuffing. An experimental and theoretical study on cam-tappet lubrication was conducted by Muller [3], focusing on cam geometry. One of the main outcomes of this study is that features of the lubricant film at the contact region need to be taken into account in the design of the cam-follower pair. Dyson [4] conducted a study focusing on assessing the lubricant film thickness and Hertzian stress along the cam operation cycle and utilizing them in the design of the cam and its follower. The load is a crucial factor in elastohydrodynamic lubrication, and it is usually difficult to calculate with a high level of accuracy. An experimental study on load measurement was presented in [5]. In this study, Bair et al fitted a force transducer on the follower in order to measure the load and friction force. Subsequently, tribology and lubrication analytical study of cams in cars was conducted by Ball [6]. An important literature review on valve train lubrication was introduced in the work of Tylor [7], which can be considered in the analysis of cam-follower lubrication. Vela et al [8] studied the non-conformal lubricated contact in the cam-follower mechanism experimentally by examining the existing optical method. This study validated the ability to utilize this apparatus in studying the contact in a cam follower pair. Wang et al. [9] studied surface waviness and its effect on eccentric-tappet lubrication. It was concluded that surface waviness results in significant effects on the characteristics of the oil film. Ciulli [10] conducted a study on a circular eccentric cam; this experimental work focused on studying eccentricity and surface roughness. The apparatus used in this study gave an encouraging outcome. Wu et al. [11] investigated the elastohydrodynamic lubrication (EHL) of the cam tappet pair, considering thermal and isothermal analysis. The results showed that the isothermal analysis gives an overevaluation of oil film thickness at certain angular positions in the cam cycle.

Al-Hamood et al. [12] carried out a numerical study of a point contact elastohydrodynamic lubrication of a cam and flat-faced follower. The study focused on studying the follower chamfering and its effect on the oil pressure and film thickness. The results indicated that the linear chamfer has a considerable effect in thinning the oil film and raising its maximum pressure. Jamali et al. [13] also presented a numerical EHL study on cam and flat-faced followers. They studied the effect of different tribological factors and geometry on oil film thickness and pressure distribution at the contact region. However, these studies considered the limited profile shape of the cam. Tang et al [14] investigated the effect of cam rotational speed in the cam-tappet mechanism on the oil film performance. They considered thermal EHL contact; the numerical model was based on the multi-grid method. A high-order polynomial cam profile was utilized. Their findings showed that decreasing the angular speed results in a reduction in film thickness and dimple depth occurred in reverse motion.

Yang et al [15] established a line contact lubrication numerical model under isothermal and thermal conditions for the cam pair used in an air splicer. The numerical solution of this model gave the pressure, film thickness, and temperature rise. Their results showed that increasing the cam base circle radius and roller radius improves the lubrication condition, while that is not the case when increasing the stroke and transition angle.

Shuyi et al [16] established a transient thermal EHL mathematical model and corresponding numerical solver for the cam roller pair in an internal combustion engine. From this study, detailed lubrication results were obtained for the cam cycle by considering actual load and other parameters from industry. The research mainly focused on investigating the lubricant film rupture and improving the pressure distribution by the effect of roller tilting and convexity. Hua et al [17] developed a mixed EHL thermal model for predicting friction and temperature at the contact zone of cam-tappet pairs. Real surface roughness and transient operational conditions were considered in this study. The heat transfer calculation was based on a fast-moving heat source condition. Their results showed that applying 3D roughness led to film thickness reduction and temperature rise, which might result in the tendency of scuffing failure. On the other hand, increasing the base circle radius and cam speed might increase the film thickness and reduce the temperature of the cam-tappet surfaces. Changing the shape of the surface is also common in other applications, such as bearings [18-22].

In elastohydrodynamic lubrication, the contacting surfaces are deformed elastically under the effect of the pressure developed at the oil film. The value and distribution of this pressure depend mainly on several factors such as the geometry of the surfaces, their velocity, and the applied load. Reducing the elastic surface deformation of the contacting surfaces is crucial in reducing the extreme stresses in the metals that lead to different types of tribological failures.

In this study, the elastohydrodynamic lubrication (EHL) of the cam follower mechanism is studied numerically, focusing on suggested geometry modifications to minimize surface deformation. The geometry is modified along the cam depth using three types of modification, which are full-depth parabola, parabolic, and linear chamfer at the edges. The resulting pressure distributions are also investigated to evaluate the effectiveness of these forms of profile.

2. DYNAMICS OF THE CAM-FOLLOWER MECHANISM

As indicated earlier, various types of cams and followers are utilized in different applications. In this study, a cam with a flat-faced follower is considered; this mechanism and the contact tangent plane are shown in Fig. 1.

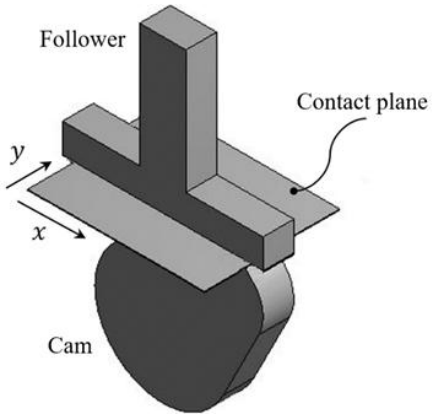

Fig. 1. Typical cam and flat face follower.

In order to investigate the elastohydrodynamic lubrication at the contact zone in the cam-follower pair, it is essential to have comprehensive knowledge of the cam and follower types under consideration. The operational conditions, such as rotational cam speed and the load applied at the follower, are also required to be determined in analysing this problem.

The cam profile is designed or selected to give the desired motion of the follower. However, this profile has a significant effect on the tribological aspects at the contact zone.

A smooth cam profile of a four-four-power polynomial Ball [6] is considered in this study. Equation (1) represents the follower lift, Lf, in terms of the cam angle of rotation, ψ, as follows,

$$L_f = Y_R + L_{f\max} + c_p\left(\frac{\psi}{\psi_T}\right)^p + c_q\left(\frac{\psi}{\psi_T}\right)^q + \\ + c_r\left(\frac{\psi}{\psi_T}\right)^r + c_s\left(\frac{\psi}{\psi_T}\right)^s \quad (1)$$

where Y_R is the ramp height, $L_{f\max}$ is the maximum value of the lift, and ψ_T is the cam half period. $p, q, r, c_p, c_q, c_r, c_s$ are parameters determine the cam features.

For the EHL computation, it is important to represent the contacting surfaces' velocity relative to the point of contact. The relative velocity for the cam and follower can be written respectively as follows:

$$u_c = \omega\left(\frac{d^2L_f}{d\psi^2} + L_f + r_B\right)$$
$$u_f = \omega\left(\frac{d^2L_f}{d\psi^2}\right) \quad (2)$$

where ω is the cam angular velocity and r_B is the base circle radius. The contacting surfaces geometries are another parameter that influences the characteristics of the lubrication in the contact zone. Accordingly, the radii of curvature of the contacting surfaces are considered together and are presented in the form of equivalent radius of curvature, R, as follows:

$$\frac{1}{R} = \frac{1}{R_c} + \frac{1}{R_f}. \quad (3)$$

R_c: the radius of curvature of the cam, and R_f: the radius of curvature of the follower. For the case studied in this research, the equivalent radius of curvature can be expressed as:

$$R = \frac{d^2L_f}{d\psi^2} + L_f + r_B. \quad (4)$$

In addition to the velocity and geometry, the load has a significant effect on the EHL performance. Generally, for the cam and its follower, the load that is developed between the contacting surfaces is accumulated from the inertia of the follower, the spring fitted to the follower to maintain contact, and the working load. The inertia and spring loads can be expressed as follows:

$$F = k\left(L_f + \delta\right) + M\omega\left(\frac{d^2L_f}{d\psi^2}\right) \quad (5)$$

where: k: spring constant; δ: spring initial deflection; M: follower mass; $\left(\frac{d^2L_f}{d\psi^2}\right)$: follower acceleration.

3. EHL MODELLING AND SOLUTION

The point contact model is built to analyze the elastohydrodynamic lubrication problem considered in this study. In this model, the coupled method is applied to the Reynolds equation and film thickness equation. In an x-y plane tangent to the contacting surfaces at the point of contact, the quasi-steady-state solution for these equations can be written as [23]:

$$\frac{\partial}{\partial x}\left(\kappa_x\frac{\partial p}{\partial x}\right) + \frac{\partial}{\partial y}\left(\kappa_y\frac{\partial p}{\partial y}\right) - \\ -\frac{\partial}{\partial x}\left(\rho\bar{u}h\right) - \frac{\partial}{\partial y}\left(\rho\bar{v}h\right) = 0 \quad (6)$$

and

$$h(x,y) = g(x,y) + \delta(x,y) + h_o. \quad (7)$$

Where; $\bar{u} = \frac{u_c + u_f}{2}$

$\bar{v} = 0$, where the cam and follower velocities are zero in the transverse direction.

u_c and u_f are presented in equation (2).

For Newtonian behaviour, the flow factors can be written as:

$$\kappa_x = \kappa_y = \frac{\rho h^3}{12\eta}. \quad (8)$$

For calculating these factors, Johnson and Tevaarwerk [24] relation of non-Newtonian oil behaviour is applied; this relation can be written as:

$$\frac{\partial u}{\partial z} = \frac{\tau_o}{\eta}\sinh\left(\frac{\tau}{\tau_o}\right). \quad (9)$$

where:

τ: Shear stress

τ_o: Non-Newtonian parameter

In order to represent the oil viscosity as a function of pressure, the equation of Roeland [25] is used. For an isothermal solution, the following equation can be written as given by Lugt and Morales [26]:

$$\eta = \eta_o exo\left\{\left[\ln\left(n_o\right)+9.67\right]\left[\left(1+\frac{p}{1.962\cdot10^8}\right)^z - 1\right]\right\} \quad (10)$$

where, $z = \frac{1.962\cdot10^8\,\alpha}{\ln\left(\eta_o\right)+9.67}$.

The oil density relation, which includes the effect of pressure given by Dowson and Higginson [27], is used in this study:

$$\rho = \rho_o \left(1 + \frac{\beta_p}{1+\phi_p} \right). \quad (11)$$

The gap between the contacting surfaces should be presented first in the EHL solution. In any non-conformal contacting surfaces, the gap depends on their equivalent radius of curvature. This was given in equation (3) for the un-modified cam and flat-faced follower. Accordingly, for this case, the gap can be written as follows [28]:

$$g = \frac{x^2}{2R}. \quad (12)$$

In order to enhance the life of the contacting surface, it is important to minimize the deformations of surfaces during passing them through the EHL contact. In this study, surface deformation is examined under three types of modifications along the cam depth, which are illustrated in Fig. 2. The cam surface along its depth (y-direction) is modified into a parabolic or linear chamfer at the edges or a full parabolic shape along the whole depth. The surface deformation is determined through the EHL solution for these suggested modifications.

As can be seen in Fig. 2, e is the chamfer height and L_c is its depth. C_r represents the chamfer depth ratio as follows:

$$C_r = \frac{L_c}{L/2}. \quad (13)$$

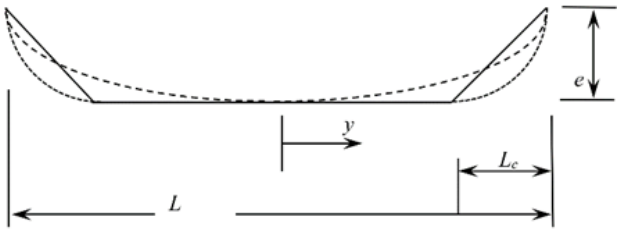

Fig. 2. Cam depth under three types of modifications. Solid: linear chamfer, dotted: parabolic chamfer, dashed: full-depth parabolic.

This ratio can be varied from 0 (no modification) to 1 (full-depth modification). It should be noted that the full-depth modification only utilizes a parabolic shape. Accordingly, the film thickness gap related to cam depth modification can be written as:

$$g_2 = \frac{\left(y - \left(L/2 - L_c \right) \right)^n}{L_c^2} e. \quad (14)$$

$n=1$ for linear chamfer, $n=2$ for parabolic chamfer. Hence, the total gap will be the sum of the gaps in Eq. (12) and (14):

$$g(x,y) = g_1 + g_2. \quad (15)$$

The surface deformation of the contacting surfaces also contributes to the thickness of the lubricant film, it is given by [28]:

$$\delta(\xi,\vartheta) = \frac{2}{\pi E'} \iint \frac{p(\xi,\vartheta)}{\sqrt{(x-\xi)^2 + (y-\vartheta)^2}} dxdy. \quad (16)$$

where, ξ and ϑ define the location of the point under consideration in the x and y coordinates, respectively.

$$\frac{2}{E'} = \frac{1-\nu_c^2}{E_1} + \frac{1-\nu_f^2}{E_2}. \quad (17)$$

E : modulus of elasticity, υ : Poisson's ratio.

The numerical solution in this study utilizes the method of central difference for the Rynolds equation discretization; the whole system of equations of the EHL solution is then ready to be solved numerically. In order to select the appropriate mesh density in the solution, different mesh size was examined in both x and y directions in the solution domain. In this mesh density test, the number of nodes k_x and k_y are increased gradually until the calculated minimum film thickness becomes almost unaffected. Accordingly, for the cases studied in this paper, it is found that the appropriate mesh density is $k_x = 362$ and $k_y = 272$ where the number of total nodes is $362 \cdot 272 = 98464$ nodes.

In order to achieve convergence of the numerical EHL solution, the calculated load is compared with the load that is applied to the contact region. The calculated load is achieved by pressure integration over the solution domain. The converging process is mainly controlled by varying the value of h_o which is a part of the lubricant film thickness as given in equation (7). The h_o varying is continued during the execution process until convergence is achieved.

4. RESULTS

In order to study the contacting surfaces undergoing elastohydrodynamic lubrication, it is important to focus on the region with the severe tribological conditions. For the cam and flat-faced follower investigated in this research, the sliding velocity between the contacting surfaces varies over the cam angle of rotation, ψ. The sliding velocity is equal to $\left(v_c - v_f\right)$ that calculated using equation (2), where these velocities belong to instantaneous points on the cam and follower surfaces adjacent to the contact point. This is shown in Fig. 3 in polar coordinates with respect to the cam angle, ψ. Noting that the dynamics of the case considered in this study are based on the data of Harrison [29]. In Fig. 3, It can be seen that the maximum sliding velocity arises at $\psi = 0°$ (at cam nose) where this is taken into account in the EHL analysis in this research.

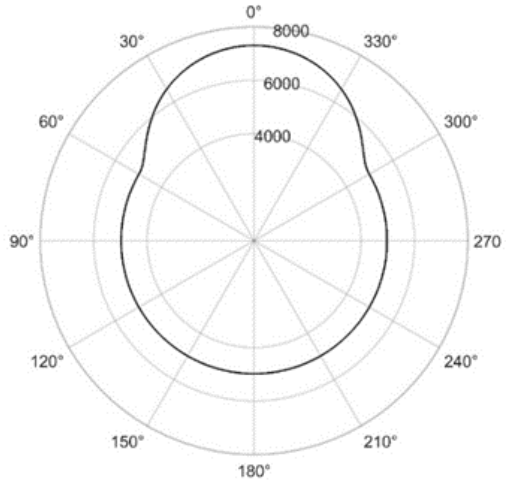

Fig. 3. The sliding velocity between the cam and follower (mm/s).

The equivalent radius of curvature of the contacting surfaces plays an important factor in the EHL regime, as described earlier, it can be calculated using equation (4). This can be depicted in Fig. 4.

In Fig. 4, it can be noted that the maximum value of the equivalent radius arises on both sides of the flank at an angle $\psi = 57.4°$ and $302.6°$, and it has a minimum value at $\psi = 0°$. This needs to be considered in the computation and analysis of the EHL solution.

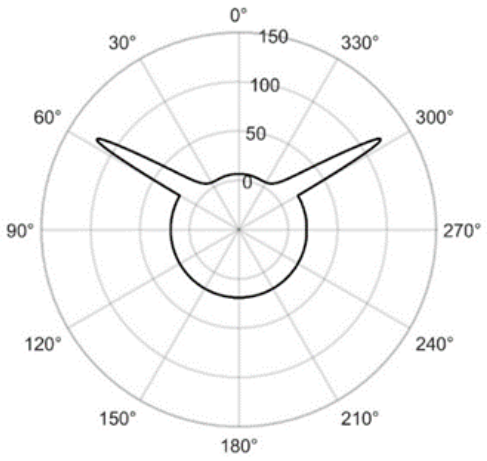

Fig. 4. Cam and follower equivalent radius of curvature (mm).

The load at the contact region also has a crucial effect on the EHL results, this is represented in equation (5) and is depicted in Fig. 5. In this figure, it can be seen similar behavior to that in Fig. 4 where the minimum value at the cam nose ($\psi = 0°$) and maximum value at both sides of the flank at $\psi = 57.4°$ and $302.6°$.

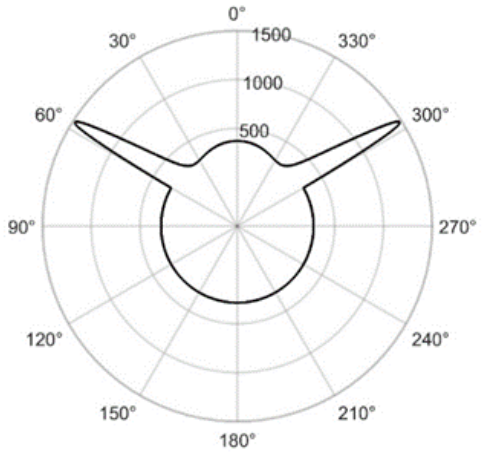

Fig. 5. The contact load (N).

Table 1 illustrates a comparison between the results of the current work with the results of the well-known approximation equation presented in Ref. [30], which is given by,

$$H_{\min} = 3.63G^{0.49}U^{0.68}W^{-0.073}\left(1 - e^{-0.68k}\right). \quad (17)$$

It is worth mentioning that. $H_{\min}$ in this equation represents the minimum film thickness is represented in a dimensionless form, while the results in Table 1 are given in its dimensional form (μm) after performing the required calculations. The case of full parabolic shape is used in this comparison, which produces an

elliptic contact problem. Four positions are used in this comparison, which are ψ=0°, ψ=20°, ψ=40°, and ψ=50. It can be seen that the maximum difference is about 6 %.

Table 1. Validation of the current model considering the minimum film thickness.

Angle	H_{min} (μm) Equation of [30]	H_{min} (μm) Current work	% Diff.
0	0.081	0.085	4.68
20	0.078	0.083	6.06
40	0.029	0.027	-5.55
50	0.649	0.610	-5.95

A full numerical EHL solution is carried out for the contact problem at the two values of cam angle: $\psi = 0°$ and $\psi = 57.4°$. Fig. 6 shows a comparison between the pressure distributions at these positions using the three geometrical modification forms shown in Fig. 2, using $e = 10$ μm. Figs 6 (a), (b), and (c) illustrate this comparison for the linear, full-depth (parabolic curve), and parabolic chamfers, respectively. It can be seen that the contact width (x - direction) is relatively larger when $\psi = 57.4°$ which is attributed to the higher value of the radius of relative curvature at this position as illustrated previously in Fig. 4.

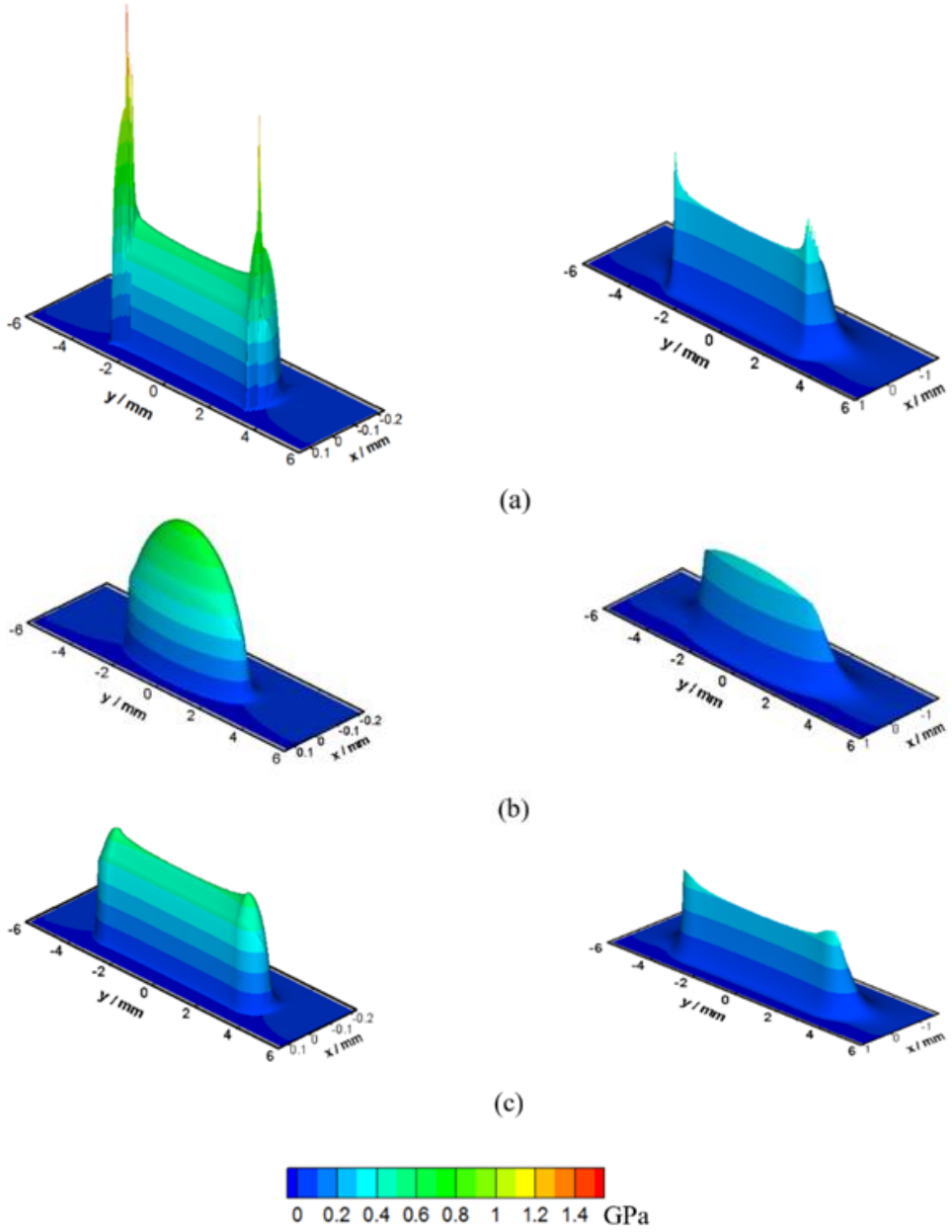

Fig. 6. Pressure distribution at ψ=0 (left) and ψ=57.4 (right) using: (a) linear chamfer, (b) full-depth parabolic, and (c) parabolic chamfer.

The generation of pressure over a wider area (for the same length) results in lower pressure values which is the case in all the three forms of modification. The linear chamfer results in higher levels of pressure, and pressure spikes occur at the start of profile change. These spikes take place due to the slope discontinuity in the surface profile. The maximum pressure values at these spikes are 1.61 GPa and 0.448 GPa when $\psi=0°$ and $\psi=57.4°$ respectively. This high level of pressure is reduced significantly when the full parabolic curve is used for the surface profile, as shown in Fig. 6 (b). The corresponding maximum pressure values become 0.74 GPa and 0.37 GPa, respectively. Due to maintaining the continuity of slope at the modification start point. However, the contact length (y- y-direction) is reduced as the pressure is not generated due to the relatively wider gap between the contacted surface, resulting from the whole-width modification. The pressure levels are further decreased when the change in the profile takes place over a portion of the width rather than the whole width in the form of a parabolic shape. In this case, the slope continuity is maintained, which helps in avoiding the presence of a large pressure spike, and also the contact length becomes longer, which produces a larger supporting area for the applied load as shown in Fig. 6 (c). The maximum pressure values become 0.55 GPa and 0.35 GPa $\psi=0°$ and $\psi=57.4°$ respectively. This represents a substantial enhancement in the EHL performance of the cam-follower pair. The consequences of this improvement on the elastic deformation of the contacted surface will be discussed later.

As mentioned previously, the major objective of this research is to examine the transverse geometry modifications of the contacting surfaces and their effect in minimizing elastic deformation during EHL contact. The pressure distributions at the contact zone shown previously in Fig. 6 for the three suggested modifications are reflected directly on the surfaces' elastic deformation. Fig. 7 shows the deformation of the contacted surfaces for $\psi=0°$ in the direction of the cam depth, y, at $x=0$. In this figure, it is apparent that the full-depth parabolic has a deformation of a maximum value of about 2.75 μm, which is much higher than the two other modifications, where they have maximum values of about 1.8 μm and 1.6 μm for linear and parabolic chamfers, respectively. Fig. 8 shows the surface deformation along the entrainment direction, x, for $y=0$ at the same cam angle $\psi=0°$. A similar comparison can be noticed as in Fig. 7.

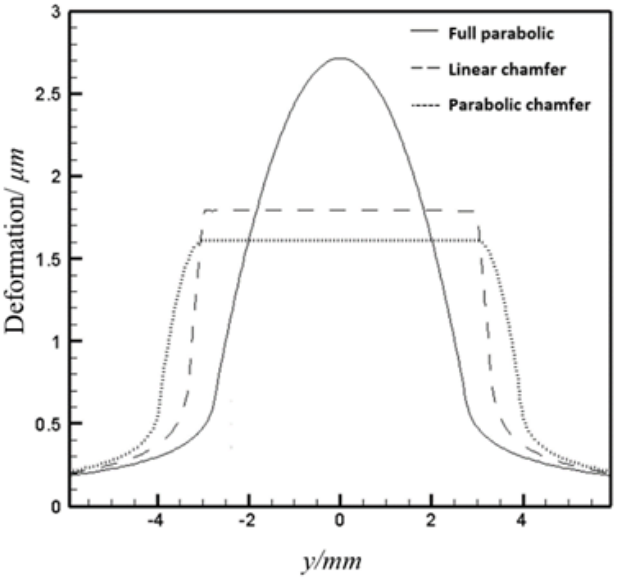

Fig. 7. The surface deformation along the transverse direction, *y* for ψ=0°.

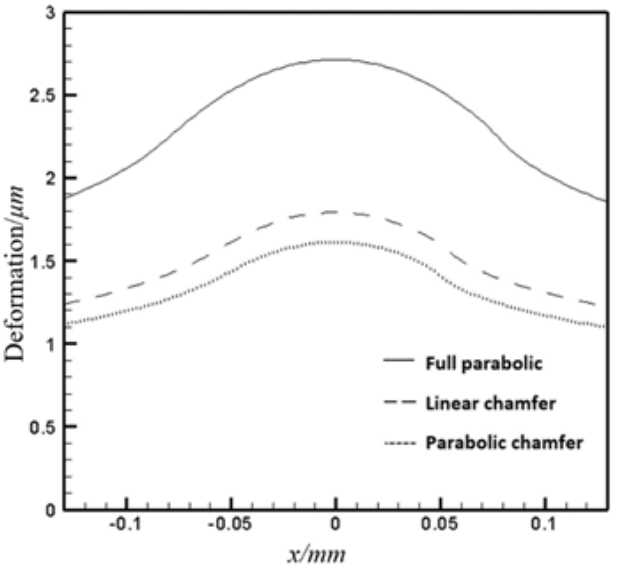

Fig. 8. Surfaces deformation along entrainment direction, *x* for ψ=0°.

A Two-dimensional representation of the surface deformation along the x and y directions for the three types of modifications is shown in Fig. 9.

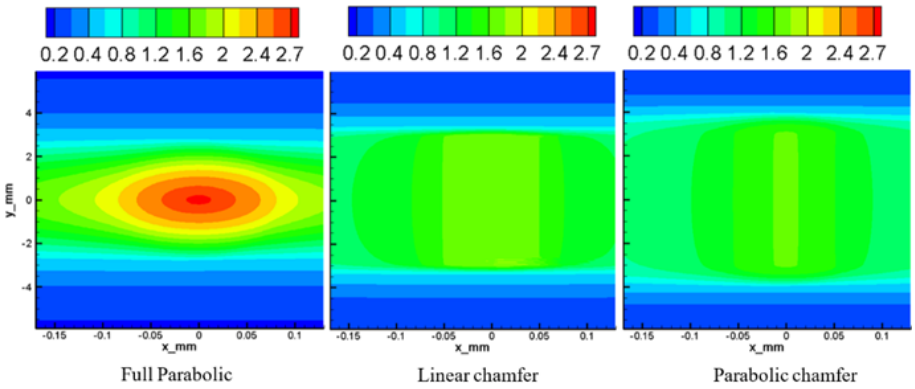

Fig. 9. Two-dimensional representation of the surface deformation along *x* and *y* directions at ψ=0°.

When the cam angle $\psi = 57.4°$, a maximum load of 1500 N is noticed along the full cam cycle. This position is considered in the calculation of the surface deformation, which is represented along the cam depth, *y*, and entrainment direction, *x*, as shown in Figs. 10 and 11, respectively. In these figures, the deformation shown is about double that in Figs. 7 and 8 due to the amount of applied load. However, similar to the previous case, the full parabolic surface encountered higher surface deformation while the parabolic chamfer produced minimum surface deformation. The parabolic chamfer is the best form in minimizing the surface deformation, resulting in about 3.8 μm maximum deformation in comparison with 4.3 μm and 5.1 μm when the linear chamfer and whole parabolic profile are used, respectively. A Two-dimensional representation of the surface deformation along the *x* and *y* directions for the three types of modifications at this position can be seen in Fig. 12.

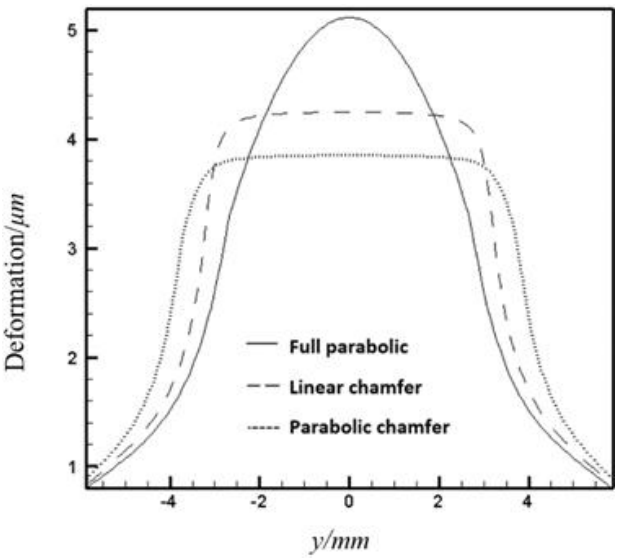

Fig. 10. The surfaces deformations along the transverse direction, *y* for ψ=57.4°.

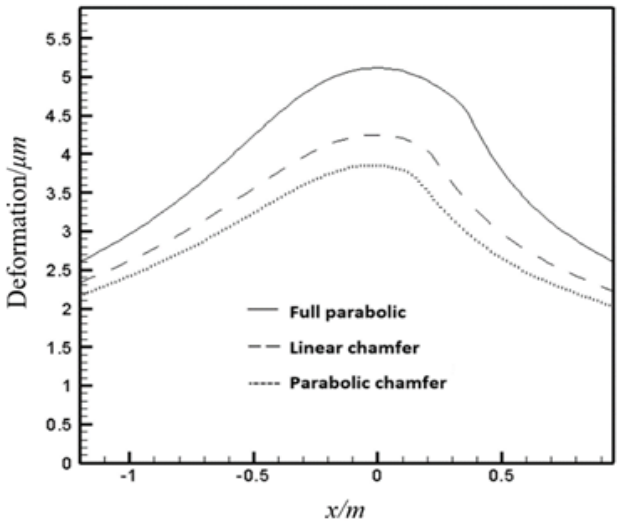

Fig. 11. The surfaces deformations along the entrainment direction *x* for ψ=57.4°.

Table 2 shows more details about the results at another three positions (ψ=20°, ψ=40°, and ψ=50°) in addition to the previous two positions (ψ=0° and ψ=57.4°). This table compares the maximum pressure and maximum deformation values at these five positions for the three types of profiles. It can be seen that the parabolic chamfer results in the lowest maximum pressure and the lowest maximum deformation at each position in comparison with the other two profile forms.

A further significant matter is the fatigue life of the mechanical elements subjected to cyclic loading, which is the case for the cam follower mechanism. Reducing surface deformation is a critical factor in extending the component life and minimizing the possibility of fatigue failure. When the mechanical element is subjected to high repetitive cyclic load, minimizing surface deformation leads directly to a reduction in internal stress levels. Consequently, this decreases the microstructural damage accumulation over time, which reduces the risk of fatigue failure.

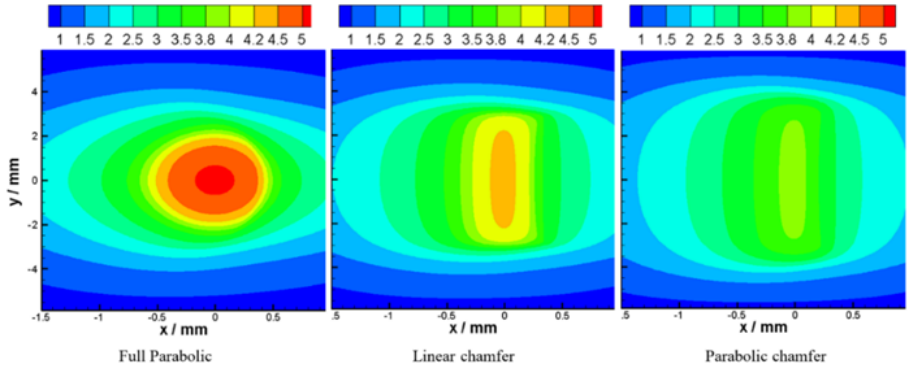

Fig. 12. Two-dimensional representation of the surface deformation along x and y directions at ψ=57.4°.

Table 2. Effect of profile shape on maximum pressure and maximum deformation values at five positions

Angle (Deg)	linear		Full parabolic		Parabolic chamfer	
	P max (GPa)	Def. max (μm)	P max (GPa)	Def. max (μm)	P max (GPa)	Def. max (μm)
0	1.6134	1.876	0.734	2.713	0.55	1.613
20	1.65	1.664	0.771	2.504	0.57	1.453
40	1.588	1.55	0.512	2.281	0.36	1.408
50	0.425	2.468	0.361	3.397	0.331	2.219
57.4	0.448	4.248	0.37	5.115	0.35	3.854

5. CONCLUSION AND REMARKS

This study investigates the effects of modifying the cam geometry on the elastic deformation of the contacted surfaces. Three types of depth modifications are examined, and the analyses are carried out at the very extreme tribological conditions (load, sliding velocity, and equivalent radius of curvature) along the cam cycle at $\psi = 0°$ and $\psi = 57.4°$. A point contact elastohydrodynamic lubrication numerical model is used to analyse the lubrication problem of the cam and flat-faced follower. Results show that the calculated deformation is affected significantly by the type of modification. The parabolic chamfer is the best form in minimizing surface deformation in comparison with the other two forms of modifications. On the other hand, the resulting pressure distribution is also related considerably to the shape of the cam depth. The linear chamfer results in significant pressure spikes due to the discontinuity in the slope of the profile. The other two forms maintain the slope continuity of the profile, which helps in avoiding large pressure spikes. However, the parabolic chamfer results in lower pressure levels; therefore, it is recommended to be used in modifying the cam shape. The outcome of this work is expected to have significant positive consequences on the fatigue life of the cam-follower pair in terms of reducing the resulting stresses. These important aspects might be considered by the authors in future research.

REFERENCES

[1] H. A. Rothbart, *CAM Design Handbook*, 1st ed. New York: McGraw-Hill, 2004.

[2] A. Dyson, and H. Naylor, "Application of the Flash Temperature Concept to Cam Tappet Wear Problem," *Proceedings of the Institution of Mechanical Engineers: Automobile Division*, vol. 14, no. 1, pp. 225-280, 1960, doi: 10.1243/PIME_AUTO_1960_000_026_02.

[3] R. Muller, "The Effect of Lubrication on Cam and Tappet Performance," *Motor Tech Z*, vol. 27, no. 2, pp. 58-61, 1966.

[4] A. Dyson, "Kinematics and Wear Patterns of Cam and Follower Automotive Valve Gear," *Tribology International*, vol. 13, iss. 3, pp. 121-132, Jun. 1980, doi: 10.1016/0301-679X(80)90056-0.

[5] S. Bair, J. Griffioen, and W. Winer, "The Tribological Behavior of an Automotive Cam and Flat Lifter System," *Journal of Tribology*, vol. 108, no. 3, pp. 478-486, Jul. 1986, doi: 10.1115/1.3261246.

[6] A. Ball, "A Tribological Study of the Design and Performance of Automotive Cams," Ph.D. dissertation, Dept. Mech. Eng., University of Leeds, Leeds, UK, 1988.

[7] C. Taylor, "Valve Train - Cam and Follower: Background and Lubrication Analysis," *Tribology Series*, vol. 26, pp. 159-181, 1993, doi: 10.1016/S0167-8922(08)70011-7.

[8] D. Vela, E. Ciulli, B. Piccigallo, and F. Fazzolari, "Investigation on cam-follower Lubricated Contacts," *Proceedings of the Institution of Mechanical Engineers, Part J: Journal of Engineering Tribology*, vol. 225, no. 6, pp. 379-392, Jun. 2011, doi: 10.1177/1350650111400157.

[9] J. Wang, C. Venner, and A. Lubrecht, "Influence of Surface Waviness on the Thermal Elastohydrodynamic Lubrication of an Eccentric-Tappet Pair," *Journal of Tribology*, vol. 135, no. 2, p. 021001, Mar. 2013, doi: 10.1115/1.4023410.

[10] E. Ciulli, F. Fazzolari, and B. Piccigallo, "Experimental study on circular eccentric-cam–follower pairs," *Proceedings of the Institution of Mechanical Engineers, Part J: Journal of Engineering Tribology*, vol. 228, no. 10, pp. 1088-1098, Apr. 2014, doi: 10.1177/1350650114529943.

[11] W. Wu, J. Wang, and C. H. Venner, "Thermal Elastohydrodynamic Lubrication of an Optimized Cam–Tappet Pair in Smooth Contact," *Journal of Tribology*, vol. 138, no. 2, p. 021501, Sep. 2015, doi: 10.1115/1.4031494.

[12] A. Al-Hamood, H. U. Jamali, O.I. Abdullah, A. Senatore, and H Kaleli, "Numerical analysis of cam and follower based on the interactive design approach," *International Journal on Interactive Design and Manufacturing (IJIDeM)*, vol. 13, no. 3, pp. 841-849, Jan. 2019, doi: 10.1007/s12008-019-00544-z.

[13] H.U. Jamali, A. Al-Hamood, O.I. Abdullah, A. Senatore, and J. Schlattmann, "Lubrication Analyses of Cam and Flat-Faced Follower," *Lubricants*, vol. 7, no. 4, p. 31, Apr. 2019, doi: 10.3390/lubricants7040031.

[14] H. Tang, J. Wang, N. Sun, and J. Zhu, "Effect of Angular Speed of Cam on Oil Film Variation in the Line Contact Thermal EHL of a Cam–Tappet Pair," *Industrial Lubrication and Tribology*, vol. 72, no. 6, pp. 713–722, Jan. 2020, doi: 10.1108/ILT-08-2019-0327.

[15] F. Yang, D. Hu, X. Han, S. Zhang, and Y. Zhao, "Numerical Analysis of Elastohydrodynamic Lubrication Characteristics of the Spatial Cam Mechanism in the Air Splicer," *Journal of Mechanical Science and Technology*, vol. 36, no. 7, pp. 3597–3607, Jul. 2022, doi: 10.1007/s12206-022-0635-3.

[16] L. Shuyi, G. Feng, S. Nannan, Z. Guixiang, C. Shen, and L. Xiaoling, "Elastohydrodynamic Lubrication Analysis of Cam–Roller Pairs of Internal Combustion Engines," *International Journal of Engine Research*, vol. 24, no. 4, pp. 1374–1387, Apr. 2022, doi: 10.1177/14680874221085638.

[17] D. Hua, R. Li, X. Shi, W. Sun, F. Shi, and X. Lu, "Predictions of Friction and Temperature at Marine Cam–Tappet Interface Based on Mixed Lubrication Analysis With Real Surface Roughness," *Proceedings of the Institution of Mechanical Engineers, Part J: Journal of Engineering Tribology*, vol. 237, no. 9, pp. 1854–1867, Jan. 2023, doi: 10.1177/13506501231188758.

[18] H.U. Jamali, H.S. Sultan, O.I Abdullah, A.N Al-Tamimi, M. S. Albdeiri, A. Ruggiero, and Z. A. AL-Dujaili, "Analysis of the Performance of Chamfered Finite-Length Journal Bearings under Dynamic Loads," *Mathematics*, vol. 11, no. 3, p. 587, Jan. 2023, doi: 10.3390/math11030587.

[19] H.U. Jamali, H.S. Sultan, O.I Abdullah, A.N Al-Tamimi, L.H. Abbud, A. Ruggiero, and Z. A. AL-Dujaili, "Effect of Chamfer Form and Parameters on the Characteristics of Finite Length Journal Bearing under Impact Load," *Lubricants*, vol. 11, no. 2, p. 73, Feb. 2023, doi: 10.3390/lubricants11020073.

[20] A.A. Hamzah, A.F. Abbas, M.N. Mohammed, H.S. Aljibori, H. U. Jamali, and O.I Abdullah, "An Evaluation of the Design Parameters of a Variable Bearing Profile Considering Journal Perturbation in Rotor–Bearing Systems," *Designs*, vol. 7, no. 5, p. 116, Oct. 2023, doi: 10.3390/designs7050116.

[21] H.S. Aljibori, M.N. Mohammed, M.J. Jweeg, H.U. Jamali, O. I Abdullah, and M. Alfiras, "Rotor Response to Unbalanced Load and System Performance Considering Variable Bearing Profile," *Nonlinear Engineering*, vol. 14, no. 1, p. 20240079, Jan. 2025, doi: 10.1515/nleng-2024-0079.

[22] H.U. Jamali, H.S. Sultan, A. Senatore, Z.A. Al-Dujaili, M.J. Jweeg, A.M. Abed, and O.I Abdullah, "Minimizing Misalignment Effects in Finite Length Journal Bearings," *Designs*, vol. 6, no. 5, p. 85, Sep. 2022, doi: 10.3390/designs6050085.

[23] R. Gohar, and H. Rahnejat, *Fundamentals of Tribology*, 2nd ed. London: Imperial College Press, 2012.

[24] C. Roelands, "Correlational aspects of the viscosity-temperature-pressure relationships of lubricating oils," Ph.D. dissertation, Technical University Delft, Delft, NL, 1966.

[25] K. L. Johnson and J. L. Tevaarwerk, "Shear behaviour of elastohydrodynamic oil films," *Proceedings of the Royal Society of London a Mathematical and Physical Sciences*, vol. 356, no. 1685, pp. 215–236, Aug. 1977, doi: 10.1098/rspa.1977.0129.

[26] P. M. Lugt, and G. E. Morales-Espejel, "A Review of Elasto-Hydrodynamic Lubrication Theory," *Tribology Transactions*, vol. 54, no. 3, pp. 470-496, Mar. 2011, doi: 10.1080/10402004.2010.551804.

[27] D. Dowson, and G. *Higginson, Elastohydrodynamic Lubrication. Pergamon*, Oxford, 1966.

[28] K. Johnson, *Contact Mechanics. Cambridge*, Cambridge University Press, 1985.

[29] P. Harrison, "A Study of Lubrication of Automotive Cams," Ph.D. dissertation, Dept. Mech. Eng., University of Leeds, Leeds, UK, 1985.

[30] A.A. Lubrecht, C.H. Venner, and F. Colin, "Film Thickness Calculation in Elasto-Hydrodynamic Lubricated Line and Elliptical Contacts: The Dowson, Higginson, Hamrock contribution," *Proceedings of the Institution of Mechanical Engineers, Part J: Journal of Engineering Tribology,* vol. 223, no. 3, pp. 511–515, Jan. 2009, doi: 10.1243/13506501JET508.